THE JOURNAL OF BIOLOGICAL CHEMISTRY VOL. 285, NO. 25, pp. 19259–19266, June 18, 2010

Phosphatidylinositol 4,5-Bisphosphate Activates Slo3 Currents and Its Hydrolysis Underlies the Epidermal Growth Factor-induced Current Inhibition*[S]

Received for publication, January 5, 2010, and in revised form, March 20, 2010 Published, JBC Papers in Press, April 14, 2010, DOI 10.1074/jbc.M109.100156

Qiong-Yao Tang[‡], Zhe Zhang[‡], Jingsheng Xia[§], Dejian Ren[§], and Diomedes E. Logothetis[‡1]

From the [‡]Department of Physiology and Biophysics, School of Medicine, Virginia Commonwealth University, Richmond, Virginia 23298-0551 and the [§]Department of Biology, University of Pennsylvania, Philadelphia, Pennsylvania 19104

The *Slo3* gene encodes a high conductance potassium channel, which is activated by both voltage and intracellular alkalinization. Slo3 is specifically expressed in mammalian sperm cells, where it gives rise to pH-dependent outwardly rectifying K^+ currents. Sperm Slo3 is the main current responsible for the capacitation-induced hyperpolarization, which is required for the ensuing acrosome reaction, an exocytotic process essential for fertilization. Here we show that in intact spermatozoa and in a heterologous expression system, the activation of Slo3 currents is regulated by phosphatidylinositol 4,5-bisphosphate (PIP_2). Depletion of endogenous PIP_2 in inside-out macropatches from *Xenopus* oocytes inhibited heterologously expressed Slo3 currents. Whole-cell recordings of sperm Slo3 currents or of Slo3 channels co-expressed in *Xenopus* oocytes with epidermal growth factor receptor, demonstrated that stimulation by epidermal growth factor (EGF) could inhibit channel activity in a PIP_2-dependent manner. High concentrations of PIP_2 in the patch pipette not only resulted in a strong increase in sperm Slo3 current density but also prevented the EGF-induced inhibition of this current. Mutation of positively charged residues involved in channel-PIP_2 interactions enhanced the EGF-induced inhibition of Slo3 currents. Overall, our results suggest that PIP_2 is an important regulator for Slo3 activation and that receptor-mediated hydrolysis of PIP_2 leads to inhibition of Slo3 currents both in native and heterologous expression systems.

The *Slo3* gene encodes a member of the high conductance potassium (Slo) family that is activated by both voltage and intracellular alkalinization (1–3). Slo3 was first cloned in 1998. Unlike Slo1, which is widely distributed in many different tissues (*e.g.* see Refs. 4–6), Slo3 was found to be expressed exclusively in mammalian testis (1). Slo3 showed greater sensitivity than Slo1 channels to intracellular tetraethylammonium, 4-aminopyridine, and intracellular and extracellular quinidine. However, no specific blocker has been reported thus far for Slo3 currents (7). Because of its sensitivity to both pH and voltage, Slo3 has been thought to be involved in sperm capacitation and/or the acrosome reaction, steps essential in mammalian fertilization (reviewed in Refs. 8–10). These two key events required for sperm to fertilize an egg involve changes in ionic permeability, intracellular pH, membrane potential, and concentrations of Ca^{2+} ($[Ca^{2+}]_i$) and cAMP (11).

Whole-cell voltage clamp recording on mouse spermatozoa revealed that an outwardly rectifying K^+ current (I_{KSper}), with properties most similar to those of mSlo3, is one of the two predominant currents in mammalian spermatozoa (12). This channel was activated by intracellular alkalinization, such as can be induced by exposure to NH_4Cl. This NH_4Cl-induced K^+ conductance controlled membrane potential and was thought to play a role in capacitation, hyperactivated motility, and the acrosome reaction in sperm cells (for a review, see Ref. 13). Slo3 has a relatively low selectivity for K^+ over Na^+ (P_K/P_{Na} ~5). As the Na^+/K^+ concentration ratio changes throughout the female reproductive tract, the channel can exert a depolarizing or a hyperpolarizing effect on sperm (11). Recently, it was shown that Slo3 knock-out mice had impaired sperm motility and were male infertile with a capacitation-induced depolarization in the mutant rather than hyperpolarization as seen in the wild type. Mutant sperm failed to undergo the acrosome reaction (14). In addition, the Slo3 mutant sperm lacked the NH_4Cl-induced outwardly rectifying K^+ currents, providing strong evidence that Slo3 underlies the Ksper currents in normal sperm (14).

Phosphatidylinositol 4,5-bisphosphate (PIP_2)[2] is a major signaling phospholipid in the inner leaflet of the plasma membrane. Most types of ion channels and ion transporters require PIP_2 to function and can be inhibited by signaling pathways that deplete or hydrolyze PIP_2 (15, 16). It has been known that, in mouse sperm, phosphoinositide-dependent pathways play an essential role in the early events of mammalian fertilization (17). Extensive studies with members of the Kir channel subfamily (Kir 1–7) have provided molecular insight into the mechanisms of the regulation of channel activities by PIP_2 (18). The direct interaction between the negative phosphate headgroups of PIP_2 and the positively charged residues in the N and C termini is essential for activation of PIP_2-sensitive channels

* This work was supported, in whole or in part, by National Institutes of Health Grants HL059949 and HL090882 (to D. E. L.). This work was also supported by discretionary institutional funds (to D. E. L.).

[S] The on-line version of this article (available at http://www.jbc.org) contains supplemental Fig. 1.

[1] To whom correspondence should be addressed. Fax: 804-828-7382; E-mail: delogothetis@vcu.edu.

[2] The abbreviations used are: PIP_2, phosphatidylinositol 4,5-bisphosphate; PIP_3, phosphatidylinositol 1,4,5-trisphosphate; EGF, epidermal growth factor; EGFR, epidermal growth factor receptor; Wtmn, wortmannin; TEVC, two-electrode voltage clamp recording; MΩ, megaohms; poly-K, polylysine; AASt, arachidonylstearyl; Ab, antibody; diC_8, 8-carbon-long acyl chain; Slo-WT, wild type Slo; mSlo, mouse Slo; n_H, Hill coefficient.

(19–23). Recent work has reported that Slo1 was directly regulated by PIP_2 (24). It was not known, however, whether PIP_2 also modulates the activity of other Slo family members, such as Slo3.

The epidermal growth factor (EGF) family has been shown to play an important role in the regulation of reproductive function. EGF is widely distributed along the reproductive tract. It has been proposed to be involved in the regulation of sperm motility (25, 26). The EGF receptor (EGFR) is localized in the flagellum and was found to be present in all non-capacitated, capacitated, and acrosome-reacted spermatozoa in humans, rabbits, and rats (27). In boars, EGFR was also localized in the flagellum, but its presence was reported to be restricted only to acrosome-reacted spermatozoa (28). Thus, EGF may act to increase sperm motility, particularly following the acrosome reaction. Because EGF is also present in oocytes, it could serve as an important co-factor in sperm activation during fertilization. Previous work has shown that stimulation of mouse spermatozoa with EGF results in PIP_2 hydrolysis, DAG generation, and acrosomal exocytosis (29). However, the mechanism of the EGF action remains unknown.

In the present study, we present evidence implicating PIP_2 as an important regulator for Slo3 activation and linking the EGF receptor-mediated inhibition of Slo3 currents to PIP_2 hydrolysis both in mouse spermatozoa and in a heterologous expression system.

EXPERIMENTAL PROCEDURES

Oocyte Preparation and Molecular Biology—Xenopus laevis oocytes were prepared and injected using standard protocols (30). Mouse Slo3 cDNA was amplified with PCR from a clone purchased from Open Biosystems and cloned into the *Xenopus* oocyte expression vector pXoom, 3′ of the T7 promoter. RNA for each channel was made using the Ambion mESSAGE mACHINE T7 kit. Mutations were made using PCR with *Pfu* polymerase and were confirmed by sequencing. The cRNA was injected at 5–15 ng/35–60 nl for two-electrode voltage clamp recording (TEVC) or 8–30 ng/50–100 nl for macropatch recording or was co-expressed with EGFR cRNAs in the ratio of 1:1.5 for TEVC recording.

Electrophysiological Macropatch Recording in Oocytes— Channel activity was recorded with devitellinized oocytes under a standard excised inside-out patch-clamp configuration (31) with an Axopatch 200 amplifier (Molecular Devices, Sunnyvale, CA). pClamp (Molecular Devices) was used to drive stimulus protocols and digitize currents. To eliminate contamination from endogenous Cl^- channels reported in oocytes, currents were all recorded in Cl^- free solutions in both the intracellular and extracellular sides. To minimize the possible contamination from endogenous Ca^{2+} (or Ca^{2+}-regulated) ion channels in oocytes, 2 mM $MgCl_2$ was used in the extracellular side of a standard pipette solution. The standard pipette solution contained 140 mM potassium methanesulfonate, 20 mM KOH, 10 mM HEPES, 2 mM $MgCl_2$, pH 7.0. The composition of solutions used to bathe the cytoplasmic face of patch membranes was 140 mM K-methanesulfonate, 20 mM KOH, 10 mM HEPES, 5 mM EGTA with pH adjusted to the values as indicated in the text and figures. Recordings were performed 4–5 days following injection. The recording pipettes used had a resistance of 0.3–0.8 MΩ in the bath solution. Currents were elicited by voltage stimuli lasting 100 ms, delivered every 1 s with a voltage ramp protocol from −100 to +160 mV. The anti-PIP_2 antibody, polylysine (poly-K), neomycin, arachidonylstearyl (AASt) PIP_2, and short chain (8-carbon-long acyl chain, diC_8) PIP_2 were applied to the intracellular side of excised patches. All experiments were performed at room temperature (~22–25 °C).

TEVC—TEVC recordings in *Xenopus laevis* oocytes were performed 3–5 days after cRNA injection (GeneClamp500 amplifier, Axon Instruments). Electrodes were filled with 3 M KCl dissolved in 1% agarose. The standard bath solution was the same as that used in the pipette solution for macropatch in Cl^- free solutions. Microelectrodes had a resistance of 0.3–1.0 MΩ. Whole-cell currents were elicited by voltage stimuli lasting 0.8 s, delivered every 5 s with a voltage ramp protocol ranging from −100 to +160 mV. Wortmannin treatment involved incubation of oocytes for 2 h before recording.

Patch-Clamp Recordings in Spermatozoa—Recordings were performed on sperm cells from the corpus epididymis derived from mice 4–11 months of age. Patches were targeted at the sperm cell cytoplasmic droplet (a thickening along the cytoplasmic tail) for cell-attached and whole-cell recordings as described previously (32, 33). Pipette resistances were 7–11 MΩ for both cell-attached and whole-cell recordings. After break-in, access resistance in the whole-cell configuration was 30–85 MΩ. Whole-cell currents were elicited by voltage stimuli lasting 0.5 s, delivered every 2–5 s with a voltage ramp protocol ranging from −100 to +160 mV. All recordings were performed at room temperature. Seals between the patch pipette and the cytoplasmic droplet were formed in HS bath solution, which contained 2 mM $CaCl_2$ to inhibit $I_{CatSper}$ reported in sperm (12, 32, 34) (135 mM NaCl, 5 mM KCl, 2 mM $CaCl_2$, 1 mM $MgSO_4$, 20 mM Hepes, 5 mM glucose, 10 mM lactic acid, 1 mM sodium pyruvate, pH 7.4, with NaOH). The osmolarity of the solution was about 300–310 mOsM/kg. The standard pipette solution was the same as that used in the intracellular side for the conventional macropatch configuration expressed in oocytes. pH was adjusted to 6.1, and osmolarity was adjusted to 285–295 mOsm/kg with glucose.

Lipid Handling, PIP_2 Dose Response and Other Chemicals— Stock solutions of AASt PIP_2 (0.5 mM) (Roche Applied Science) in different pH solutions were prepared by sonication in cold water or on ice for more than 25 min and kept at −80 °C. The working solutions were prepared by diluting the stock solution to the desired concentrations, followed by at least 25 min of additional sonication. diC_8 PIP_2 (purchased from Avanti) was dissolved in the desired experimental solution at a concentration of 500 mM with pH adjusted to the nominal values as indicated in the text and figures and stored at −80 °C. Further dilutions were made to the desired pH solution. Stocks and working solutions of other chemicals, such as PIP_2 antibody (Avanti), poly-K (Sigma), wortmannin (Sigma), and EGF (Roche Applied Science) were prepared using protocols according to the manufacturer's instructions. The pH of the stock solution for each chemical was adjusted to the nominal values as indicated in the text and figures.

Data Analysis—Currents obtained at +160 mV (averaged over a 5–20-ms duration) were plotted as a function of time. Signals were acquired in pClamp 9 (Axon Instruments). Signals were filtered at 2 kHz and sampled at 10 kHz. The current size and its activation or inhibition were measured at +160 mV. The Hill equation was used to fit Figs. 2*F* and 3*B*, and the Boltzmann equation was used to fit Fig. 1*E* (Origin 7.0, Microcal Software). Data are expressed as mean ± S.E. Statistical comparisons were made with a two-tailed *t* test (Origin 7.0); $p < 0.05$ indicated statistical significance.

RESULTS

Depletion of Endogenous PIP$_2$ Inhibits Slo3 Channels Expressed in Xenopus Oocytes—We first tested whether Slo3 currents were sensitive to PIP$_2$ scavengers. In the first 1–2 min following excision into inside-out macropatches, ~90% of recordings showed weak run down of channel activity. As has been shown for other channels, activity run down is likely to result from a gradual depletion of membrane PIP$_2$ following patch excision. Weak run down may reflect relatively strong binding between endogenous PIP$_2$ and Slo3 channels. To test for this possibility, we applied PIP$_2$ antibody (PIP$_2$ Ab) into the bath solution. Slo3 currents induced by high pH (pH 8.5) were greatly inhibited by PIP$_2$ Ab, (1:100 dilution), resulting in an 86.0 ± 1.6% inhibition ($n = 10$) (Fig. 1, *A–C*). This inhibitory effect could be partially reversed by further perfusion of 5 μM PIP$_2$ AASt. The average recovery current level by PIP$_2$ was 61.7 ± 3.2% ($n = 4$). The proportion of the current gradually activated by PIP$_2$ is likely to reflect a corresponding increase in rebinding of PIP$_2$ to channels. The kinetic process of reactivation by PIP$_2$ was fitted with a single exponential function, and the T_{50} (time required for half-maximal activation) was 216.3 ± 29.2 s ($n = 4$) (Fig. 1*A*).

Next we tested the effects of wortmannin (Wtmn) on Slo3 currents. Wtmn, which is known to block the activity of most phosphatidylinositol 3-kinases at nanomolar concentrations, also blocks 4-kinases at micromolar concentrations (35), thus reducing resynthesis of PIP$_2$ to the plasma membrane. TEVC recordings demonstrated that Slo3 currents expressed in oocytes were greatly inhibited by pretreatment with 30 μM Wtmn for 2 h ($n = 6$; Fig. 1, *D* (*right panels*) and *E*). Uninjected control oocytes showed little detectable currents ($n = 11$) and no effect by a 2-h pretreatment of Wtmn ($n = 9$; Fig. 1, *D* (*left panels*) and *E*). The conductance (*G*)-voltage relationships demonstrated that the inhibition of Slo3 currents by Wtmn was weakly voltage-dependent (Fig. 1*E*).

Positively charged poly-K acts as a PIP$_2$ scavenger that inhibits the activities of several PIP$_2$-sensitive ion channels (*e.g.* see Refs. 20 and 36). Application of 300 μg/ml poly-K (M_r ~8000 Da) resulted in fast inhibition of Slo3 currents (inhibition 77.3 ± 0.9% ($n = 33$)). As was the case following inhibition by PIP$_2$ Ab (Fig. 1*A*), AASt PIP$_2$ gradually reactivated Slo3 currents (62.9 ± 2.1%, $n = 3$) (Fig. 2, *A–C*), presumably reflecting an increase in rebinding of exogenous PIP$_2$ to the channel. Similarly, application of neomycin, a polycation that reversibly complexes membrane PIP$_2$ (37) and prevents it from interacting with the channel, resulted in a fast and stepwise reduction in channel activity. The estimated IC$_{50}$ for neomycin inhibition

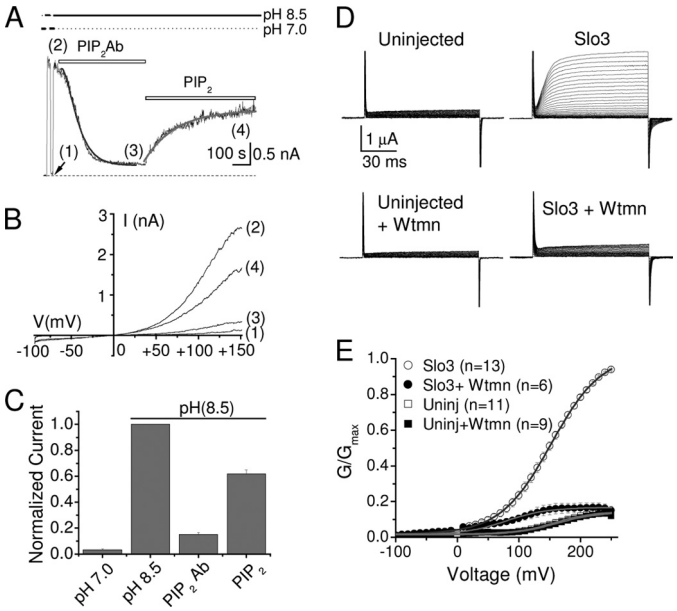

FIGURE 1. **Reducing endogenous PIP$_2$ levels by PIP$_2$ Ab or Wtmn inhibits Slo3 channels expressed in *Xenopus* oocytes.** *A*, representative time course of an inside-out macropatch recording from oocytes injected with Slo3 cRNA. The experiment shows current block by PIP$_2$ Ab (1:100), followed by partial reactivation by 5 μM AASt PIP$_2$. A monoexponential fit to the time course of recovery from PIP$_2$ Ab inhibition is shown. T_{50} value during PIP$_2$ reactivation represents the time required to reach 50% of the steady-state current level (216 ± 29 s, mean ± S.E. ($n = 4$)). The PIP$_2$ Ab inhibition showed faster kinetics than the PIP$_2$ reactivation (55 ± 6 s, mean ± S.E. ($n = 6$)). Current sizes were measured at +160 mV (see "Experimental Procedures"). The *dashed line* represents zero current level. The *horizontal bars above* indicate the changes in intracellular pH$_i$ between 7.0 and 8.5. *B*, representative Slo3 currents evoked by a 100-ms voltage ramp ranging from −100 to +160 mV at the time points indicated by *numbers* in *A*, to show the effect of alkalinization (from *1* to *2*), inhibition by PIP$_2$ Ab (*3*), and reactivation by PIP$_2$ (*4*). Traces are averaged from 10 runs. *C*, *bars* represent normalized currents (at +160 mV) induced by alkalinization (from pH 7.0 to 8.5), inhibition by PIP$_2$ Ab, and reactivation by PIP$_2$ (at pH 8.5). Data points represent mean ± S.E. (*error bars*) of at least four experiments. Currents were normalized to the level after alkalinization at an intracellular pH of 8.5. *D*, whole-cell currents (TEVC) were obtained using voltage steps (100 ms) in increments of 10 mV starting from a holding potential of −100 mV to +250 mV. *Left*, uninjected oocytes with (*below*) or without (*above*) a 2-h preincubation with Wtmn. *Right*, currents from Slo3-injected oocyte with (*below*) or without (*above*) 2-h preincubation with Wtmn. *E*, averaged conductance-voltage relationships for uninjected and Slo3-expressing oocytes in the presence and absence of preincubation with Wtmn. The two curves for uninjected oocytes (*open* and *filled squares*) overlap.

was 0.53 ± 0.04 mM with a Hill coefficient (n_H) of 0.9 ± 0.1 (n = 10; Fig. 2, *D–F*). Removal of neomycin induced a quick recovery, suggesting rapid PIP$_2$ rebinding with the channel (Fig. 2, *D* and *E*). The fast reactivation upon washout of neomycin suggests that neomycin acts as a weaker PIP$_2$ scavenger than poly-K, following washout of which there was little recovery. The relatively weaker PIP$_2$ scavenging ability of neomycin *versus* poly-K not only reflects the fact that neomycin is less positively charged (+6) than poly-K (≫6) but also is consistent with the hypothesis that the Slo3 channel is likely to bind PIP$_2$ more strongly than other channels, such as Kir1.1 channels. With Kir1.1 channels, increases of neomycin concentrations resulted in a fast and stepwise reduction in channel activity with an IC$_{50}$ of 0.2 ± 0.1 mM and a complete inhibition at 5 mM (38). The higher IC$_{50}$ for Slo3 reflects its stronger binding with PIP$_2$ compared with Kir1.1 channels. Consistent with this interpretation, >30 mM neomycin was required to produce a complete inhibition of Slo3 currents (Fig. 2, *D–F*).

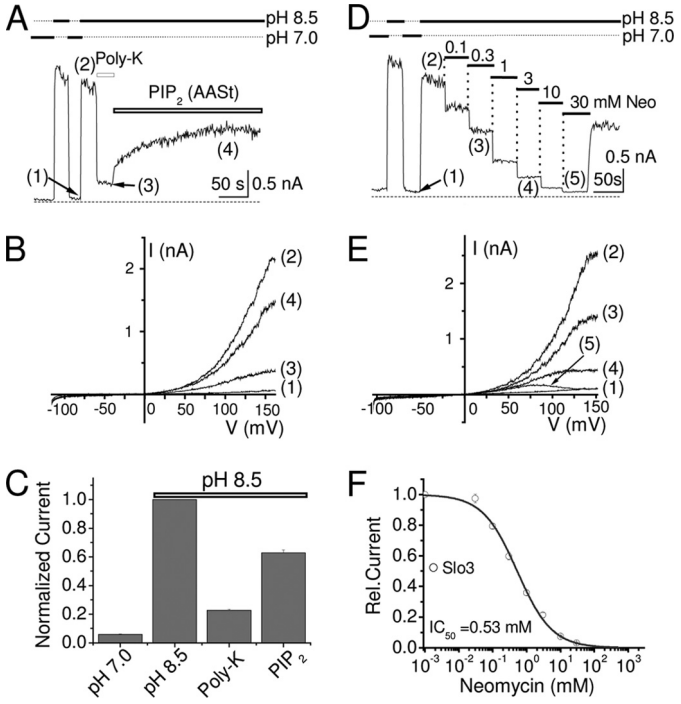

FIGURE 2. **Depletion of endogenous PIP$_2$ level by poly-K or neomycin (*Neo*) inhibits Slo3 channel-PIP$_2$ interactions in *Xenopus* oocytes.** *A*, representative time courses of recordings from oocytes injected with Slo3 showing current block by 300 μg/ml poly-K and reactivation by AASt PIP$_2$ (5 μM or higher concentrations). Current amplitudes were measured at +160 mV (see "Experimental Procedures"). The *dashed line* indicates the zero current level. The *horizontal bars above* indicate the changes in intracellular pH$_i$ between 7.0 and 8.5. *B*, representative Slo3 currents evoked by a 100-ms voltage ramp ranging from −100 to +160 mV at the time points indicated by *numbers* in *A*, to show the effect of alkalinization (from *1* to *2*), inhibition by poly-K (*3*), and reactivation by PIP$_2$ (*4*). Traces are averages from 10 runs. *C*, bars represent normalized currents (at +160 mV) induced by alkalinization (from pH 7.0 to 8.5), inhibition by poly-K, and reactivation by PIP$_2$. Data represent mean ± S.E. (*error bars*) of 3–8 experiments. Currents were normalized to the level following alkalinization at a pH of 8.5. *D*, representative time course recording from oocytes injected with Slo3 showing rapid inhibition by various concentrations of neomycin and partial recovery by washout. Current amplitudes were measured at +160 mV. The *dashed line* represents the zero current, and *horizontal bars above* indicate the changes in intracellular pH between 7.0 and 8.5. *E*, representative Slo3 currents evoked by a 100-ms voltage ramp ranging from −100 to +160 mV at the time points indicated by *numbers* in *D*, to show the effect of alkalinization (from *1* to *2*) and inhibition by different concentrations of neomycin (0.3 mM (*3*), 3 mM (*4*), and 30 mM (*5*)). Traces are averages from six runs. *F*, dose-response curves for inhibition of Slo3 channels by neomycin fitted to a standard Hill function with an IC$_{50}$ = 0.53 ± 0.04 mM and Hill coefficient of 0.9 ± 0.1. Data points represent mean ± S.E. (*error bars*) of n = 10. Notice that some of the error bars are smaller than the open circles.

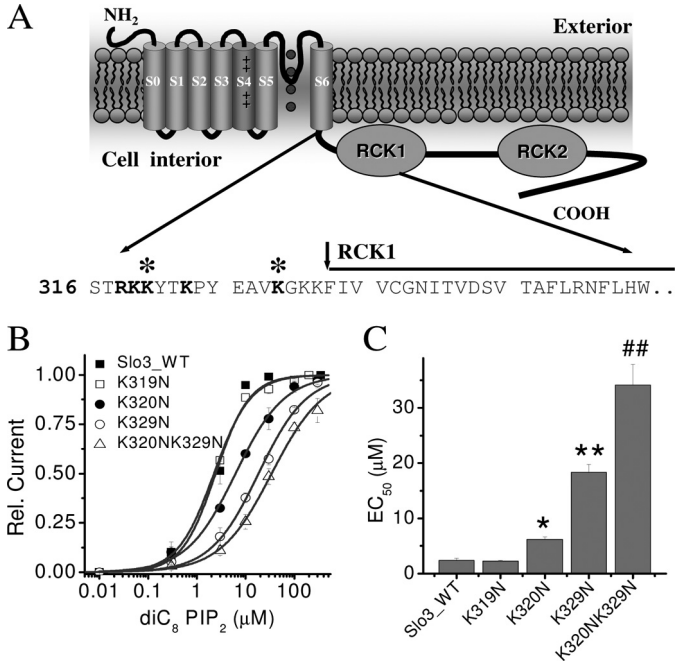

FIGURE 3. **Mutations of positively charged residues in a carboxyl intracellular domain decrease the apparent channel-PIP$_2$ affinity.** *A*, mutated positive charged residues clustered at the intracellular mouth of Slo3 channels are shown in *boldface letters*. The *asterisks* denote residues whose mutation affected the apparent PIP$_2$-channel affinity (PIP$_2$ interaction sites; see *B*). The *arrows* indicate the start of the juxtamembrane domain and within the RCK1 domain, respectively, in the Slo3 C terminus. *B*, relative currents ($I_{diC8\text{-}PIP2}/I_{max}$) in response to diC$_8$-PIP$_2$ application subsequent to the endogenous PIP$_2$ depletion by poly-K (300 μg/ml) for Slo3-WT and mutant channels. Curves were fitted to a standard Hill function with an EC$_{50}$ and Hill coefficient, respectively, of 2.4 ± 0.3 μM and 2.11 for wild type, 6.2 ± 0.5 μM and 0.9 for K320N, 18.4 ± 1.4 μM and 0.9 for K329N, and 34.6 ± 4.4 μM and 0.8 for K320N/K329N. Data points represent mean ± S.E. (*error bars*) of 3–7 determinations. *C*, bars represent averaged EC$_{50}$ values of diC$_8$ PIP$_2$ responses for Slo3-WT and mutants. ##, $p < 0.001$; **, $p < 0.005$; *, $p < 0.05$.

Residues in the Slo3 Cytosolic C Terminus That Affect Channel-PIP$_2$ Interactions—In general, channel-PIP$_2$ interactions have been shown to be electrostatic in nature (39, 40). The positively charged cytoplasmic residues clustered close to the bottom of the pore-forming S6 (or M2) segments in PIP$_2$-sensitive channels have been shown to be critical for the PIP$_2$ action (*e.g.* see Refs. 20 and 41). The region near the intracellular mouth of Slo3 channel was screened for residues that might contribute electrostatically to the binding of PIP$_2$ (shown in boldface type in Fig. 3*A*). We proceeded to test whether neutralization mutations would cause a decrease in the apparent affinity of the channel for PIP$_2$. We used a synthetic water-soluble analog of PIP$_2$, diC$_8$ PIP$_2$, that enabled us to construct dose-response relationships (*e.g.* see Refs. 20 and 41) (Fig. 3*B*).

Following channel activation by intracellular alkalinization (pH 8.5), poly-K was applied (300 μg/ml) to inhibit Slo3 currents. Then different concentrations of diC$_8$ PIP$_2$ at pH 8.5 were applied to reactivate Slo3 currents. Dose-response curves were fitted by the Hill equation for the wild-type Slo3 (Slo3-WT) and carboxyl terminal mutants made within the juxtamembrane region, where basic residues have been shown to interact with PIP$_2$ in other ion channels. The EC$_{50}$ for activation of Slo3-WT by diC$_8$ PIP$_2$ was 2.4 ± 0.3 μM with a Hill coefficient of 2.1 (n = 4–5) (Fig. 3*B*). The summarized data of EC$_{50}$ values for various mutations are shown in Fig. 3*C*. Thus, both the K320N (EC$_{50}$ = 6.2 ± 0.5 μM; n_H = 0.9; n = 4–6) and K329N (EC$_{50}$ = 18.4 ± 1.4 μM; n_H = 0.9; n = 4–6) mutations significantly reduced the sensitivity of the channel to activation by PIP$_2$, suggesting that both of these residues may be involved in direct channel-PIP$_2$ interaction. Furthermore, the double mutant K320N/K329N largely decreased the sensitivity of the Slo3 channel to PIP$_2$ activation (EC$_{50}$ = 34.6 ± 4.4 μM; n_H = 0.8; n = 3–7; Fig. 3, *B* and *C*). In contrast, the mutants K319N and K323N (data not shown) showed sensitivity to diC$_8$ PIP$_2$ that was indistinguishable from that of the wild-type channel. These results implicated the Lys^{320} and Lys^{329} residues of the channel's juxtamembrane cytosolic domain to be involved in channel activation by PIP$_2$.

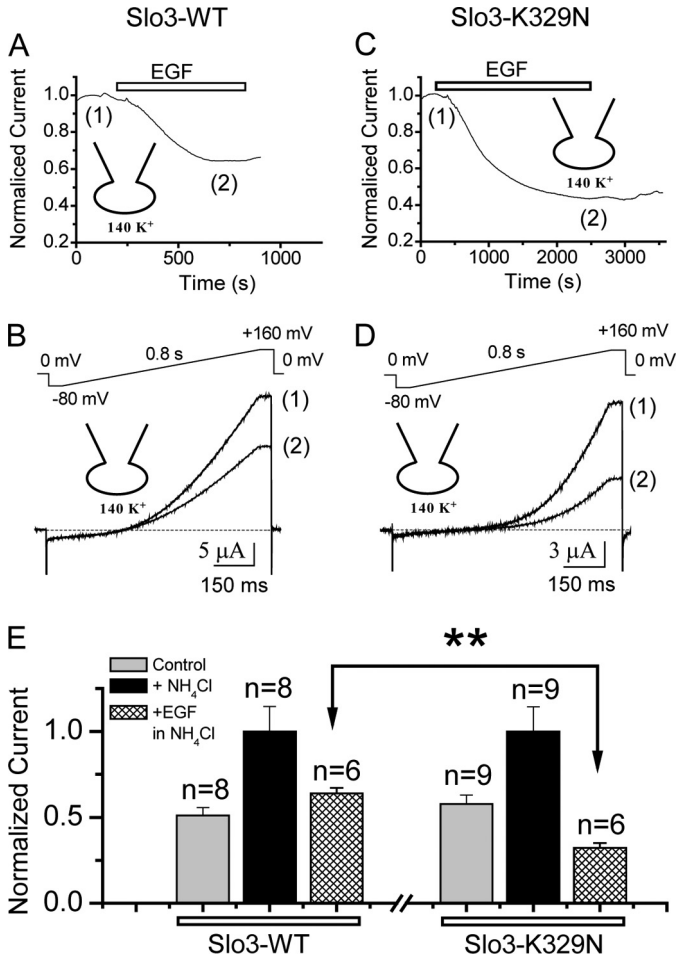

FIGURE 4. **The apparent affinity of channel-PIP$_2$ interactions determines the degree of EGF-induced inhibition of Slo3 channels expressed in *Xenopus* oocytes.** *A*, time course recording of channel inhibition by EGF for Slo3-WT channels following intracellular alkalinization induced by adding 15 mM NH_4Cl to the bath. Slo3-WT was co-injected with EGFR in oocytes. Currents were measured at +160 mV (see "Experimental Procedures"). *B*, representative whole-cell currents (TEVC) of Slo3-WT co-injected with EGFR in oocytes. Currents were evoked by a 0.8-s voltage ramp protocol ranging from −80 to +160 mV at the time points indicated by the *numbers* in *A*. *C*, similar to *A* but with the Slo3-K329N mutant. *D*, similar to *B*, but with the Slo3-K329N mutant. *E*, *bars* represent normalized currents induced by intracellular alkalinization by adding NH_4Cl to the bath and inhibition by EGF (+NH_4Cl) for Slo3-WT (*left*) and Slo3-K329N (*right*) currents. Current amplitudes were normalized to the levels after alkalinization induced by adding 15 mM NH_4Cl to the bath (**, $p < 0.005$). *Error bars*, S.E.

Growth Factor Receptor Stimulation Inhibits the Slo3-WT and K329N Mutant Channels to Different Extents—It has been known that, in *Xenopus* oocytes, stimulation of EGFR by EGF can initiate PIP_2 hydrolysis through receptor tyrosine kinase activation of PLCγ (42), such that it causes inhibition of K^+ currents (*e.g.* see Ref. 43). We proceeded to compare the effects of receptor-induced inhibition on Slo3-WT *versus* Slo3-K329N mutant, which significantly decreased channel-PIP_2 interactions. We co-expressed EGFR either with Slo3-WT (Fig. 4, *A*, *B*, and *E* (*left*)) or with the Slo3-K329N mutant (Fig. 4, *C*, *D*, and *E* (*right*)) channels in *Xenopus* oocytes and assessed the relative inhibition by EGF. Whole-cell TEVC indicated that stimulation of EGFR by EGF resulted in slightly higher inhibition for the K329N mutation (29.6 ± 2.2% inhibition, $n = 4$) compared with Slo3-WT channels (20.4 ± 1.5% inhibition, $n = 4$). However, following intracellular alkalinization induced by 15 mM NH_4Cl in the bath, the relative EGF-induced inhibition was significantly greater for the K329N mutant (67.7 ± 2.8% inhibition, $n = 6$) compared with 36.0 ± 3.1% inhibition for wild-type channels ($n = 6$) (Fig. 4*E*). This result suggested that the extent of inhibition by EGF depends on the relative strength of channel-PIP_2 interactions. The enhanced EGF-induced inhibition following alkalinization reflects an interesting pH_i dependence, the mechanism for which remains unknown.

PIP_2 Increases Sperm Slo3 Current Density—Northern blot analysis and reverse transcription-PCR experiments have suggested that Slo3 is specifically expressed in testis in both mice and humans (1). Although the lack of specific Slo3 antibodies has prevented immunocytochemical identification and localization of mSlo3, whole-cell recordings from intact sperm have revealed an outwardly rectifying K^+ current, specifically localized to the principal piece of the sperm flagellum, that has been thought to be the most likely candidate responsible for sperm Slo3 currents (12). However, these currents under the recording conditions employed do not exhibit the time or voltage dependence seen in the mSlo3 currents heterologously expressed in *Xenopus* oocytes (12).

We set out to compare K^+ currents recorded in spermatozoa with Slo3 currents expressed in oocytes under a higher voltage recording protocol (~+160 mV) than employed previously (see "Experimental Procedures" and supplemental Fig. 1). After alkalinization induced by NH_4Cl externally in the bath, the currents (in symmetrical 140 mM [K^+]) elicited with a voltage ramp protocol from −100 to +150 mV from intact sperm show that the sperm Slo3 currents steeply rectify (supplemental Fig. 1*B*). In step depolarizations, the currents elicited at higher voltage steps from +100 to +160 mV revealed a weak voltage and time dependence (supplemental Fig. 1*D*). Moreover, a current-voltage profile similar to that of Slo3 expressed in oocytes was obtained (supplemental Fig. 1, *A* and *C*; see "Discussion"). However, the native current displayed a relatively stronger activation by alkalinization at pH 6.1 (before application of NH_4Cl; see supplemental Fig. 1*B*) than mSlo3 expressed in *Xenopus* oocytes (supplemental Fig. 1*B*). One possible reason for this difference could be due to differences in intracellular modulators of Slo3 in the two expression systems. Modulators of Slo3 currents remain largely unexplored. For example, a recent study showed that the β4 subunit of Slo1 is abundantly expressed in both testes and sperm and that co-expression of this subunit in *Xenopus* oocytes produced an 8–9-fold enhancement of Slo3 currents (44).

Next, we proceeded to test whether sperm Slo3 currents exhibited a similar dependence on PIP_2 as did the heterologously expressed channel. Inclusion of PIP_2 into the recording pipette did not show an effect in the cell-attached configuration (Fig. 5, *A* and *B* (*left*)) but largely increased the current density in whole-cell recordings from intact spermatozoa (Fig. 5, *A* and *B* (*middle* and *right*)). The averaged sperm Slo3 current density increased 8.6-fold when 200 µM diC_8 PIP_2 was included in the pipette as compared with when it was not ($n > 7$; Fig. 5, *A* and *B* (*middle*)). Intracellular alkalinization, induced by the addition of 10 mM NH_4Cl in the bath, strongly potentiated sperm Slo3 current density in both cases, with or without PIP_2 in the

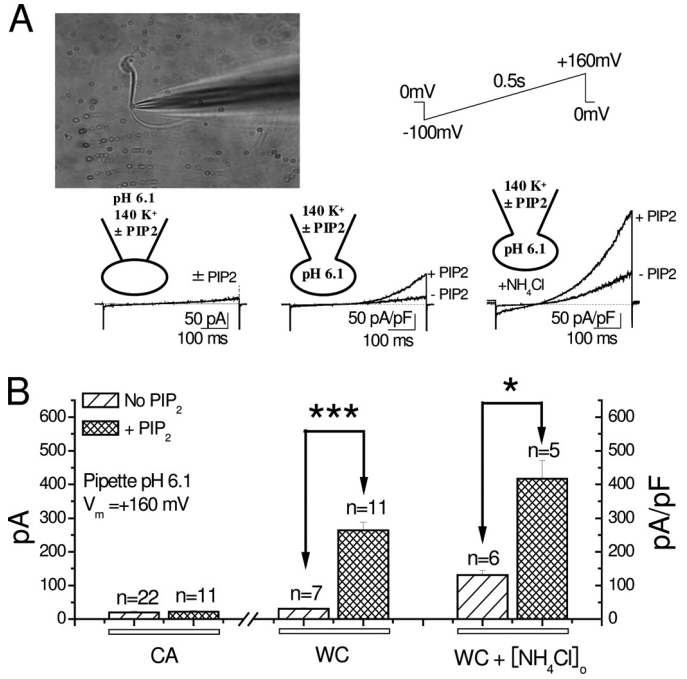

FIGURE 5. **Intracellular PIP$_2$ increases sperm Slo3 current density.** *A*, representative sperm Slo3 current in cell-attached (*CA*; *left*) or whole-cell recording configurations in sperm before (*WC*; *middle*) and after intracellular alkalinization induced by adding NH_4Cl to the bath (*WC* + $[NH_4Cl]_o$; *right*). A 0.5-s voltage ramp was applied from −100 to +160 mV with or without diC_8 PIP_2 in the pipette solution. Shown is a patch pipette attached to the membrane on the cytoplasmic droplet of a sperm cell. *B*, *bars* represent sperm Slo3 current amplitude in cell-attached (*left*) or current densities before (*middle*) and after (*right*) intracellular alkalinization induced by adding NH_4Cl to the bath, with or without diC_8 PIP_2 in the pipette solution. Data points represent mean ± S.E. (*error bars*) of at least five experiments. ***, $p < 0.0001$; *, $p < 0.01$.

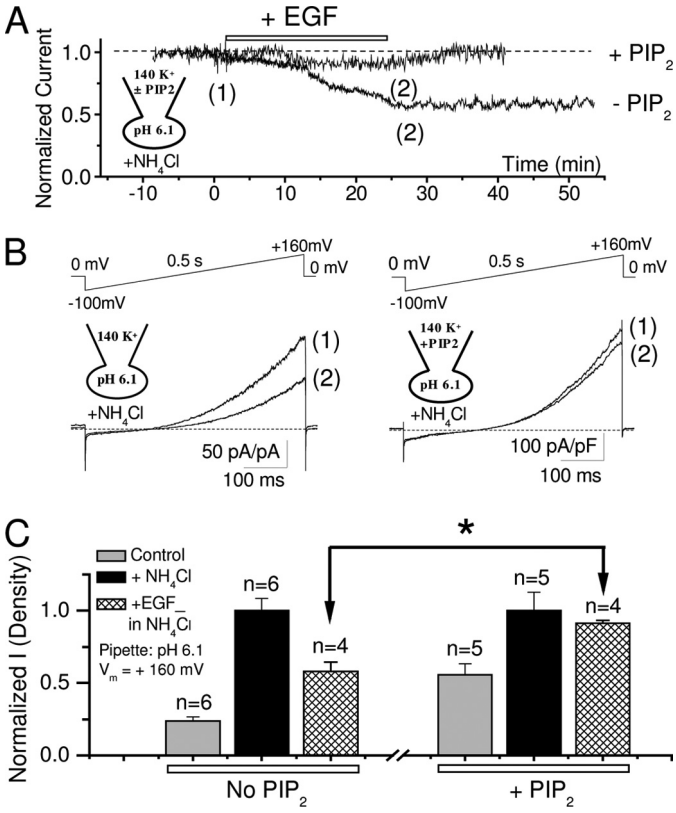

FIGURE 6. **Intracellular PIP$_2$ prevents sperm Slo3 current inhibition by EGF in whole-cell patch-clamp recordings.** *A*, time courses of representative whole-cell recordings showing that EGF inhibited the native current, but such an inhibition was prevented by inclusion of diC_8 PIP_2 in the recording pipette. Current amplitudes were measured at +160 mV (see "Experimental Procedures") and normalized to the maximum after intracellular alkalinization by adding NH_4Cl to the bath. *B*, representative sperm Slo3 current densities evoked by a 0.5-s voltage ramp from −100 to +160 mV at the time points indicated by the *numbers* in *A*, to show the effect of diC_8 PIP_2 present in the pipette solution (*right*) on the EGF-induced current inhibition compared with the absence of diC_8 PIP_2 from the pipette solution (*left*). Current amplitudes were normalized to the levels after induction of alkalinization by the addition of 15 mM NH_4Cl to the bath. *, $p < 0.005$. *C*, *bars* represent normalized current densities induced by intracellular alkalinization by the addition of NH_4Cl to the bath and inhibition by EGF application to the bath (in the presence of NH_4Cl) with (*right*) or without (*left*) diC_8 PIP_2 in the pipette solution (*, $p < 0.01$). Currents were measured at +160 mV and normalized to the level following intracellular alkalinization by the addition of NH_4Cl to the bath solution. *Error bars*, S.E.

pipette solution (Fig. 5, *A* and *B*, *right*). In the presence of 10 mM NH_4Cl (Fig. 5, *A* and *B* (*right*)), the averaged sperm Slo3 current density was increased 3.2-fold by inclusion of PIP_2 in the pipette. These results demonstrate that intracellular PIP_2 activated sperm Slo3 currents directly in spermatozoa. Several conductances have been described in sperm (45), and as such, the question arises of whether PIP_2 potentiates other currents that contribute to the outwardly rectifying K^+ currents we recorded. Because the Slo3 knock-out showed that the NH_4Cl-induced outwardly rectifying K^+ currents were due to Slo3, we proceeded to test the effects of EGF on NH_4Cl-induced Slo3 currents in sperm.

Epidermal Growth Factor Receptor Stimulation Inhibits Sperm Slo3 in the Absence but Not in the Presence of Exogenous PIP$_2$—We next tested whether sperm Slo3 was regulated by EGF. Application of EGF (150 nM) to the bath solution in a whole-cell recording of sperm partially inhibited the currents (41.9 ± 6.5%, $n = 4$) following current activation by 10 mM NH_4Cl (Fig. 6, *A–C*), suggesting a possible role for current inhibition by PIP_2 hydrolysis. The inclusion of 200 μM diC_8 PIP_2 in the recording pipette solution prevented the EGF inhibitory effect (8.7 ± 6.1%, $n = 4$) (Fig. 6, *A–C*). These results suggest that PIP_2 hydrolysis caused by EGFR stimulation regulates sperm Slo3 currents. Because EGF causes PIP_2 hydrolysis and acrosomal exocytosis in sperm (29), it is likely that the sperm Slo3 current inhibition caused by PIP_2 depletion contributes to the acrosome reaction.

DISCUSSION

PIP_2 has been shown to be a necessary cofactor for the activity of many ion channels. Recent studies have suggested that a plethora of regulatory factors (such as polyamines, kinases, pH, and Na^+ ions) that modulate Kir channel activity are coupled to PIP_2 sensitivity (46–48). In the present study, we have characterized the effects of PIP_2 on Slo3 channels. Our data provide strong evidence that PIP_2 may serve indeed as an important regulator of Slo3 channel activity both in a heterologous expression system and in native mammalian sperm. We identified two residues in the cytoplasmic C-terminal juxtamembrane region that are likely to be involved in direct channel-PIP_2 interactions, as in other channels (*e.g.* see Refs. 36, 49, and 50). In addition, our results suggest that PIP_2 hydrolysis through stimulation of the EGF receptor inhibits Slo3 channels expressed in both *Xenopus* oocytes and native spermatozoa.

Whole-cell recordings of sperm revealed a constitutively active, outwardly rectifying potassium current, similar to that previously reported for the Ksper current but with some distinct differences from the expressed Slo3 (12). In contrast, our study suggests strongly that Ksper and Slo3 are one and the same current. First, we show that this K^+ current is clearly activated by both voltage and intracellular alkalinization by testing a wide voltage range from −100 to +160 mV. Second, in symmetrical K^+ conditions with 2 mM $CaCl_2$ in the bath to eliminate possible contamination from monovalent currents via Catsper channels (see "Experimental Procedures"), we obtained a current using a ramp protocol ranging from −100 to +160 mV that showed a current-voltage profile similar to that obtained in *Xenopus* oocytes (supplemental Fig. 1, *B* and *D*). Furthermore, the EGF-inhibited sperm currents in step depolarizations showed both time and voltage-dependence even at lower voltages than those shown (data not shown). Similar results to ours have been reported by Martinez-Lopez *et al.* (11), who showed a time- and voltage-dependent current that responded to the Slo3 blockers in mature sperm. Thus, the whole-cell currents recorded in mouse spermatozoa under our conditions are indeed likely to represent native Slo3 currents.

PIP$_2$ Acts as an Important Regulator for Slo3 Activation Both in a Heterologous Expression System and in Native Cells—The channel-PIP$_2$ interactions appear to be direct in nature, and depletion or hydrolysis of PIP$_2$ causes current inhibition. The activation of Slo3 channels at higher pH_i (pH_i 8.5) was inhibited following the depletion of endogenous PIP$_2$ by scavengers, such as PIP$_2$ Ab, wortmannin, poly-K, and neomycin, suggesting a critical dependence of Slo3 activation on PIP$_2$. In addition, inclusion of diC$_8$ PIP$_2$ in the patch pipette increased the sperm Slo3 current density by ~8.6-fold at +160 mV (~8.2 fold at +100 mV). These results demonstrated once again the importance of PIP$_2$ in the regulation of Slo3 channel activity both in a heterologous expression system and in native mammalian sperm. On the other hand, the sequestration of endogenous PIP$_2$ with PIP$_2$ Ab (Fig. 1*A*) displayed considerably faster rates than the subsequent monoexponential reactivation rates upon application of PIP$_2$ AASt, suggesting that the rates of activation and deactivation cannot be explained by a simple bimolecular reaction scheme. Further detailed studies to examine the effects of pH_i and PIP$_2$ gating kinetics may be required to address this issue.

Two Residues Located in the C-terminal Cytosolic Juxtamembrane Region of Slo3 Channels Are Involved in Channel-PIP$_2$ Interactions—Slo3 is formed by four identical α subunits with a long cytosolic carboxy-terminal tail that has been proposed to be responsible for regulation of channel activity by ligands (52). Studies in Kir channels have revealed that the nature of channel-PIP$_2$ interaction is electrostatic (20, 53). Positive residues clustered at the C-terminal cytosolic juxtamembrane region have been shown in a number of channels to contribute to PIP$_2$ sensitivity. Our data show that neutralization of two basic residues (K320N and K329N) resulted in significant decreases ($p < 0.05$ for K320N and $p < 0.01$ for K329N) in the apparent channel-PIP$_2$ affinity, in contrast with charge neutralization of neighboring amino acids that showed no effect. In fact, neutralization mutations of either K320 or K329 yielded reduced n_H values, suggesting that at least one PIP$_2$ molecule was bound to the mutant channels compared with the wild-type (n_H ~2). Thus, allosteric mechanisms and possible conformational changes affecting interactions with PIP$_2$ at different sites are likely to be involved to explain these effects.

Slo3 channel-PIP$_2$ interactions show high affinity (diC$_8$ PIP$_2$ EC_{50} = 2.4 ± 0.3 μM at a pH of 8.5). In Kir channels, where the specificity of interactions with different stereoisomers of phosphoinositides has been studied in detail (41), it was found that channels exhibiting the highest PIP$_2$ affinity also exhibited high stereospecificity of interactions with PIP$_2$. This correlation of affinity and specificity is supported by a number of PIP$_2$-interacting proteins (41, 54). Thus, although we did not examine the Slo3-PIP$_2$ stereospecificity directly, it is likely that the high affinity of Slo3 channels for PIP$_2$ also makes them highly stereospecific in their interactions for this most abundant plasma membrane phosphoinositide. As the capacitated sperm interacts with the egg, ZP3, a glycoprotein component of the egg's zona pellucida, stimulates production of PIP$_3$, which in turn activates downstream kinases, such as Akt and PKCζ. This pathway is critical for triggering the acrosome reaction and is required for successful *in vitro* fertilization (17). If indeed, Slo3 channels are stereospecific and are not activated by PIP$_3$, then the PIP$_3$ production from PIP$_2$ during ZP3 stimulation would serve to inhibit Slo3 and depolarize the sperm membrane, also helping to trigger the acrosome reaction.

EGF Regulation through PIP$_2$ Hydrolysis Acts as a Native Regulator in Sperm—Our results show that PIP$_2$ hydrolysis through stimulation of EGFR inhibits Slo3 currents in both a heterologous expression system and in native mammalian sperm. It has been shown that EGF plays an important role in regulating reproductive function by increasing sperm motility. In this study, we have shown that EGF stimulation resulted in K^+ current inhibition regardless of whether it was tested with Slo3 in a heterologous expression system or with sperm Slo3 currents in native mouse sperm. Decreasing channel-PIP$_2$ interactions through mutagenesis of critical channel residues that decrease the affinity of interactions enhanced the level of EGF-induced inhibition. Moreover, inclusion of diC$_8$ PIP$_2$ in the patch pipette attenuated the ability of EGF to inhibit NH_4Cl-induced sperm Slo3 currents (Fig. 5, *C–E*), demonstrating the significant role of PIP$_2$ in sperm Slo3 current regulation.

Because EGF stimulation has been shown to induce the acrosome reaction in sperm (51), and stimulation of spermatozoa with EGF has been shown to result in hydrolysis of PIP$_2$, it is likely that the concomitant inhibition of sperm Slo3 currents by PIP$_2$ hydrolysis would depolarize the sperm membrane and serve as a contributing factor to the Ca^{2+}-dependent exocytotic event that is characteristic of the acrosome reaction. The extent to which the sperm Slo3 current inhibition by PIP$_2$ hydrolysis contributes to extracellular calcium entry *versus* intracellular calcium release by inositol triphosphate, the product of PIP$_2$ hydrolysis, remains to be investigated.

In summary, our study explored PIP$_2$ regulation of Slo3 channels in *Xenopus* oocytes and mouse sperm Slo3 currents. Although the currents recorded from the intact spermatozoa do not match perfectly those expressed in oocytes, the recent Slo3 knock-out mouse studies lend further confidence that Slo3

underlies the alkalinization-induced K^+ current responsible for the hyperpolarization seen during capacitation. Our results showed that 1) PIP_2 acts similarly to regulate both heterologously expressed Slo3 and sperm Slo3 currents, and 2) PIP_2 hydrolysis through stimulation of EGFR underlies modulation of both of the Slo3 currents. The similar regulation of Slo3 expressed in *Xenopus* oocytes and the native currents in sperm by PIP_2 and EGF has added yet one more piece of evidence that sperm Slo3 currents are the product of Slo3 expression.

Acknowledgments—We are grateful to Heikki Vaananen, Sophia Gruszecki, and Dr. Mei Zhang for oocyte isolation. We thank Dr. Christopher J. Lingle (Washington University, St. Louis, MO) for careful reading of the manuscript and critical feedback. We are also thankful to members of the Logothetis laboratory for critical feedback on this work at every stage of its development.

REFERENCES

1. Schreiber, M., Wei, A., Yuan, A., Gaut, J., Saito, M., and Salkoff, L. (1998) *J. Biol. Chem.* **273,** 3509–3516
2. Zhang, X., Zeng, X., Xia, X. M., and Lingle, C. J. (2006) *J. Gen. Physiol.* **128,** 301–315
3. Zhang, X., Zeng, X., and Lingle, C. J. (2006) *J. Gen. Physiol.* **128,** 317–336
4. Atkinson, N. S., Robertson, G. A., and Ganetzky, B. (1991) *Science* **253,** 551–555
5. Tang, Q. Y., Qi, Z., Naruse, K., and Sokabe, M. (2003) *J. Membr. Biol.* **196,** 185–200
6. Saito, M., Nelson, C., Salkoff, L., and Lingle, C. J. (1997) *J. Biol. Chem.* **272,** 11710–11717
7. Tang, Q. Y., Zhang, Z., Xia, X. M., and Lingle, C. J. (2010) *Channels* **4,** 22–41
8. Visconti, P. E., Westbrook, V. A., Chertihin, O., Demarco, I., Sleight, S., and Diekman, A. B. (2002) *J. Reprod. Immunol.* **53,** 133–150
9. Breitbart, H. (2003) *Cell Mol. Biol.* **49,** 321–327
10. Darszon, A., Acevedo, J. J., Galindo, B. E., Hernández-González, E. O., Nishigaki, T., Treviño, C. L., Wood, C., and Beltrán, C. (2006) *Reproduction* **131,** 977–988
11. Martínez-López, P., Santi, C. M., Treviño, C. L., Ocampo-Gutiérrez, A. Y., Acevedo, J. J., Alisio, A., Salkoff, L. B., and Darszon, A. (2009) *Biochem. Biophys. Res. Commun.* **381,** 204–209
12. Navarro, B., Kirichok, Y., and Clapham, D. E. (2007) *Proc. Natl. Acad. Sci. U.S.A.* **104,** 7688–7692
13. Navarro, B., Kirichok, Y., Chung, J. J., and Clapham, D. E. (2008) *Int. J. Dev. Biol.* **52,** 607–613
14. Santi, C. M., Martínez-López, P., de la Vega-Beltrán, J. L., Butler, A., Alisio, A., Darszon, A., and Salkoff, L. (2010) *FEBS Lett.* **584,** 1041–1046
15. Suh, B. C., and Hille, B. (2005) *Curr. Opin. Neurobiol.* **15,** 370–378
16. Logothetis, D. E., Petrou, V. I., Adney, S. K., and Mahajan, R. (2010) *Pflugers Arch. Eur. J. Physiol.*, in press
17. Jungnickel, M. K., Sutton, K. A., Wang, Y., and Florman, H. M. (2007) *Dev. Biol.* **304,** 116–126
18. Logothetis, D. E., Jin, T., Lupyan, D., and Rosenhouse-Dantsker, A. (2007) *Pflugers Arch.* **455,** 83–95
19. Fan, Z., and Makielski, J. C. (1997) *J. Biol. Chem.* **272,** 5388–5395
20. Lopes, C. M., Zhang, H., Rohacs, T., Jin, T., Yang, J., and Logothetis, D. E. (2002) *Neuron* **34,** 933–944
21. Schulze, D., Krauter, T., Fritzenschaft, H., Soom, M., and Baukrowitz, T. (2003) *J. Biol. Chem.* **278,** 10500–10505
22. Shyng, S. L., Cukras, C. A., Harwood, J., and Nichols, C. G. (2000) *J. Gen. Physiol.* **116,** 599–608
23. Huang, C. L., Feng, S., and Hilgemann, D. W. (1998) *Nature* **391,** 803–806
24. Vaithianathan, T., Bukiya, A., Liu, J., Liu, P., Asuncion-Chin, M., Fan, Z., and Dopico, A. (2008) *J. Gen. Physiol.* **132,** 13–28
25. Fujita, A., Nakamura, K., Kato, T., Watanabe, N., Ishizaki, T., Kimura, K., Mizoguchi, A., and Narumiya, S. (2000) *J. Cell Sci.* **113,** 103–112
26. NagDas, S. K., Winfrey, V. P., and Olson, G. E. (2002) *Biol. Reprod.* **67,** 1058–1066
27. Furuya, S., Endo, Y., Oba, M., Ito, T., Suzuki, S., and Nozawa, S. (1993) *Nippon Sanka Fujinka Gakkai Zasshi* **45,** 1313–1319
28. Oliva-Hernández, J., and Pérez-Gutiérrez, J. F. (2008) *Theriogenology* **70,** 1159–1169
29. Murase, T., and Roldan, E. R. (1995) *FEBS Lett.* **360,** 242–246
30. Logothetis, D. E., Movahedi, S., Satler, C., Lindpaintner, K., and Nadal-Ginard, B. (1992) *Neuron* **8,** 531–540
31. Hamill, O. P., Marty, A., Neher, E., Sakmann, B., and Sigworth, F. J. (1981) *Pflugers Arch.* **391,** 85–100
32. Xia, J., Reigada, D., Mitchell, C. H., and Ren, D. (2007) *Biol. Reprod.* **77,** 551–559
33. Kirichok, Y., Navarro, B., and Clapham, D. E. (2006) *Nature* **439,** 737–740
34. Liu, J., Xia, J., Cho, K. H., Clapham, D. E., and Ren, D. (2007) *J. Biol. Chem.* **282,** 18945–18952
35. Nakanishi, S., Catt, K. J., and Balla, T. (1995) *Proc. Natl. Acad. Sci. U.S.A.* **92,** 5317–5321
36. Zhang, H., Craciun, L. C., Mirshahi, T., Rohács, T., Lopes, C. M., Jin, T., and Logothetis, D. E. (2003) *Neuron* **37,** 963–975
37. Arbuzova, A., Martushova, K., Hangyás-Mihályné, G., Morris, A. J., Ozaki, S., Prestwich, G. D., and McLaughlin, S. (2000) *Biochim. Biophys. Acta* **1464,** 35–48
38. Rapedius, M., Fowler, P. W., Shang, L., Sansom, M. S., Tucker, S. J., and Baukrowitz, T. (2007) *Neuron* **55,** 602–614
39. Ravichandran, K. S., Zhou, M. M., Pratt, J. C., Harlan, J. E., Walk, S. F., Fesik, S. W., and Burakoff, S. J. (1997) *Mol. Cell. Biol.* **17,** 5540–5549
40. Kavran, J. M., Klein, D. E., Lee, A., Falasca, M., Isakoff, S. J., Skolnik, E. Y., and Lemmon, M. A. (1998) *J. Biol. Chem.* **273,** 30497–30508
41. Rohács, T., Lopes, C. M., Jin, T., Ramdya, P. P., Molnár, Z., and Logothetis, D. E. (2003) *Proc. Natl. Acad. Sci. U.S.A.* **100,** 745–750
42. Margolis, B., Rhee, S. G., Felder, S., Mervic, M., Lyall, R., Levitzki, A., Ullrich, A., Zilberstein, A., and Schlessinger, J. (1989) *Cell* **57,** 1101–1107
43. Kobrinsky, E., Mirshahi, T., Zhang, H., Jin, T., and Logothetis, D. E. (2000) *Nat Cell Biol.* **2,** 507–514
44. Yang, C. T., Zeng, X. H., Xia, X. M., and Lingle, C. J. (2009) *PLoS One* **4,** e6135
45. Zhang, D., and Gopalakrishnan, M. (2005) *J. Androl.* **26,** 643–653
46. Suh, B. C., and Hille, B. (2008) *Annu. Rev. Biophys.* **37,** 175–195
47. Xie, L. H., John, S. A., Ribalet, B., and Weiss, J. N. (2005) *J. Gen. Physiol.* **126,** 541–549
48. Xie, L. H., John, S. A., Ribalet, B., and Weiss, J. N. (2007) *Prog. Biophys. Mol. Biol.* **94,** 320–335
49. Lopes, C. M., Remon, J. I., Matavel, A., Sui, J. L., Keselman, I., Medei, E., Shen, Y., Rosenhouse-Dantsker, A., Rohacs, T., and Logothetis, D. E. (2007) *Channels* **1,** 124–134
50. Rohács, T., Lopes, C. M., Michailidis, I., and Logothetis, D. E. (2005) *Nat. Neurosci.* **8,** 626–634
51. Lax, Y., Rubinstein, S., and Breitbart, H. (1994) *FEBS Lett.* **339,** 234–238
52. Salkoff, L., Butler, A., Ferreira, G., Santi, C., and Wei, A. (2006) *Nat. Rev. Neurosci.* **7,** 921–931
53. Zhang, H., He, C., Yan, X., Mirshahi, T., and Logothetis, D. E. (1999) *Nat Cell Biol.* **1,** 183–188
54. Rosenhouse-Dantsker, A., and Logothetis, D. E. (2007) *Channels* **1,** 189–197